Journal of Asian Earth Sciences 49 (2012) 191–202

Contents lists available at SciVerse ScienceDirect

Journal of Asian Earth Sciences

journal homepage: www.elsevier.com/locate/jseaes

Hf isotopic characteristics of the Tarim Permian large igneous province rocks of NW China: Implication for the magmatic source and evolution

Zilong Li [a,*], Yinqi Li [a], Hanlin Chen [a], M. Santosh [b], Shufeng Yang [a], Yigang Xu [c], Charles H. Langmuir [d], Zhongxing Chen [d], Xing Yu [e], Siyuan Zou [a]

[a] Department of Earth Sciences, Zhejiang University, Hangzhou 310027, PR China
[b] Department of Natural Environmental Science, Kochi University, Kochi 780-8520, Japan
[c] Guangzhou Institute of Geochemistry, Chinese Academy of Sciences, Guangzhou 510640, PR China
[d] Department of Earth and Planetary Science, Harvard University, Cambridge, MA 02138, USA
[e] Second Institute of Oceanography, State Oceanic Administrator, Hangzhou 310012, China

ARTICLE INFO

Article history:
Received 18 March 2011
Received in revised form 22 November 2011
Accepted 25 November 2011
Available online 6 January 2012

Keywords:
Geochemistry
Hf isotope
Basalt
Intrusive rock
Magma source and evolution
Tarim large igneous province
Permian

ABSTRACT

The Tarim large igneous province (TLIP) in northwestern China, covering an area of ca. 250,000 km^2, includes large volumes of basalts, basic dyke swarms, mafic-ultramafic intrusion and minor picrite. Here we report systematic Hf isotope data from basalt, diabase, olivine pyroxenite and syenitic porphyry from the TLIP and address the source components and magma evolution. The subdivision of the Tarim basalts shows that the Group 1 and Group 2 basalts are clearly differentiated based on different Nb/Y values, with two subgroups (Group 1a, Group 1b) identified based on distinct P_2O_5 vs. Mg# trends. The $^{176}Hf/^{177}Hf$ isotopic composition of the basalts ranges from 0.282584 to 0.282837. The $\varepsilon Hf(t)$ of the basalts belonging to the Group 1a, Group 1b and Group 2 are −0.4–4.4, 0.5–2.1, and 1.9–3.1, respectively, and those of the intrusive suite of olivine pyroxenite, diabase and syenitic porphyry show a range of 6.0–6.5, 4.5–5.7, and 6.5–8.3, respectively. The TLIP basalts generally show a good positive correlation between $^{176}Hf/^{177}Hf$ and $^{143}Nd/^{144}Nd$, and fall in the field of the oceanic island basalts (OIBs) with low $^{176}Hf/^{177}Hf$ and $^{143}Nd/^{144}Nd$, comparable to the basaltic lavas of the Pitcairn hotspot. These features, together with the enriched signature of the Tarim basalts might reflect the incorporation of partial melting of lithospheric mantle source in the early stages of the plume activity. The TLIP basalts show low $\varepsilon Nd(t)$ and moderate $\varepsilon Hf(t)$ OIB-like source. The $^{176}Hf/^{177}Hf$-$^{143}Nd/^{144}Nd$ values of the Group 1a and Group 1b basalts of the TLIP basalts are comparable to those from the Karoo high-Ti basalts, and those of the Group 2 basalts are comparable to the features of the Karoo low-Ti basalts and diabases. The Group 1a and Group 1b basalts fall in the same Hf–Nd array, whereas the Group 2 basalts fall in a different array with much higher $\varepsilon Nd(t)$. The olivine pyroxenite, diabase and syenitic porphyry fall in the higher $\varepsilon Nd(t)$ and $\varepsilon Hf(t)$ field, with the olivine pyroxenite and diabase having features close to OIB-like source. Our new Hf isotopic results suggest distinct sources for the Tarim basalts (285–290 Ma) and the intrusive rocks (274–284 Ma). Furthermore, the $\varepsilon Hf(t)$ vs. $\varepsilon Nd(t)$ plots show that the basalts and intrusive rocks might correspond to two different periods of magmatic activity in the Tarim Basin during the Early Permian, being comparable to the temporal evolution of different rock units in the TLIP. The $\varepsilon Hf(t)$ and $\varepsilon Nd(t)$ combined with other evidences address that the basalts could be explained by being derived from the asthenospheric (or plume) mantle and having interaction with lithospheric mantle source by mainly lower degree of partial melting in the early stage before the eruption, and should be much less proportion of crustal contamination during the period of 285–290 Ma, and the intrusive rocks might be derived from the primary magma and/or OIB-like mantle sources and underwent a magma process mainly by fractional crystallization and/or cumulation during the period of 274–284 Ma.

1. Introduction

Continental flood basalts (CFBs) and large igneous provinces (LIPs) have received considerable attentions recently in relation to mantle dynamics as well as plate and plume tectonics (Carlson et al., 2006). The continental flood-basalt volcanism has been

* Corresponding author. Address: Department of Earth Sciences, Zhejiang University, 38 Zheda Road, Hangzhou 310027, PR China. Tel./fax: +86 571 87951580.
E-mail address: zilongli@zju.edu.cn (Z. Li).

1367-9120/$ - see front matter © 2011 Elsevier Ltd. All rights reserved.
doi:10.1016/j.jseaes.2011.11.021

linked to an anomalously hot, enriched mantle reservoir (White and McKenzie, 1989), the effects of mantle flow close to the lithospheric mantle boundaries (Carlson and Hart, 1987; King and Anderson, 1998), mantle plumes (e.g., Richards et al., 1989; Campbell and Griffiths, 1990; Ernst and Buchan, 2003), and by delamination of the lower parts of continental lithosphere (e.g., Elkins-Tanton and Hager, 2000; Hales et al., 2005) under continental extensional setting (Harry and Leeman, 1995). Continental flood basalts show elemental and isotopic compositional range similar to either mid-ocean-ridge basalts (MORBs) or ocean-island basalts (OIBs) (e.g., Condie, 2001). The interaction among end-member components of mantle plume and/or asthenosphere, heated lithosphere mantle, and continental crust plays an important role for the LIPs and/or CFBs. The lithosphere can modify asthenosphere (plume)-derived melts through contaminating the melts with subcontinental lithospheric mantle and continental crust (e.g., Arndt and Christensen, 1992), and may serve as an important site of melt generation for the formation of continental flood basalt provinces (e.g., Campbell and Griffiths, 1990; Turner and Hawkesworth, 1995; Turner et al., 1996; Wang et al., 2008). Furthermore, systematic Hf isotopic study combined with Sr–Nd–Pb–Os–O isotopes and major and trace elemental data for the basalts and intrusive rocks can provide a good trace for the contributions of the magmatic source components of the end-members of the OIB-MORB-EM (enriched mantle)-DMM (depleted MORB mantle) system and even magmatic evolution of the CFBs and LIPs as well as the genetic link with mantle plume. The recent advancements in analytical techniques has led to the application of Hf-isotope geochemistry in a variety of problems related to petrogenesis and tectonics, and studies on the Lu–Hf system combined with Nd isotope compositions can provide a very good constraint on the solid earth evolution (Patchett and Tatsumoto, 1980, 1981a,b; Patchett et al., 1981; Patchett, 1983a,b; Blichert-Toft and Albarède, 1997; Salters and White, 1998; Blichert-Toft et al., 1999; Vervoort and Blichert-Toft, 1999; Blichert-Toft and White, 2001; Carlson et al., 2006; Ellam, 2006; Jourdan et al., 2007; Wang et al., 2008; Mahéo et al., 2009; Ellis et al., 2010). In this study, we focus on the Lu–Hf isotopic system because it is a sensitive monitor of source components and mineralogy, as the different chemical behavior of the parent and daughter elements results in larger variations in $^{176}Hf/^{177}Hf$ relative to $^{143}Nd/^{144}Nd$ ratios.

Permian continental flood basalts and other related igneous rocks in the Tarim Basin and surrounding regions of northwestern China have been well studied in terms of petrology, geochemistry and Sr–Nd–Pb isotopes, particularly in the Keping area of northwestern Tarim Basin (Fig. 1). The rocks constitute the ~274–290 Ma Tarim Large Igneous Province (TLIP) with a large-scale distribution of basalts (ca. 250,000 km^2), including picrite, and widely developed basic dyke swarms and coeval mafic-ultramafic intrusions as documented from the surface outcrops and drilling data (Chen et al., 1997; Jiang et al., 2004a,b, 2006; Yang et al., 2006a,b, 2007a,b; Li et al., 2008, 2011; Zhang et al., 2008, 2010; Zhou et al., 2009; Tian et al., 2010; Yu et al., 2011). The TLIP can be compared to the ~250 Ma Siberian Traps in Russia (Campbell et al., 1992; Lightfoot et al., 1993; Ivanov, 2007) and the ~258–260 Ma Emeishan LIP in southwestern China (Chung and Jahn, 1995; Xu et al., 2001; Xiao et al., 2003), with probable link to mantle plume activity (Zhang et al., 2008; Yu et al., 2009; Pirajno et al., 2009; Zhou et al., 2009; Li et al., 2011).

The Hf isotope characteristics of the various units in the TLIP have not yet been investigated in detail. In this paper, we present a detailed Hf isotope study for the 285–290 Ma basalts and 274–284 Ma intrusive rocks (olivine pyroxenite, diabase, syenite, total 32 samples) collected from the field outcrops of the Yingan (Yg), Sishichang (Ssc) and Xiahenan (Xhn) sections of Keping areas, and Xiaohaizi and Wajilitag of Bachu areas of the northwestern Tarim, the Taxinan section (Txn) of southwestern Tarim, and the Shengli (SL), Yangta (YT), He, Hadexun (H) and Yingmai (YM) drill holes of the Northern and Central Tarim Basin (Fig. 1). Rocks belonging to the 289 Ma (285–290 Ma) and 275 Ma (274–284 Ma) groups were used in the calculation of $\varepsilon Hf(t)$ and $\varepsilon Nd(t)$ because these ages represent the eruption timing of the basalts and the emplacement of the intrusive suite. The purpose of our

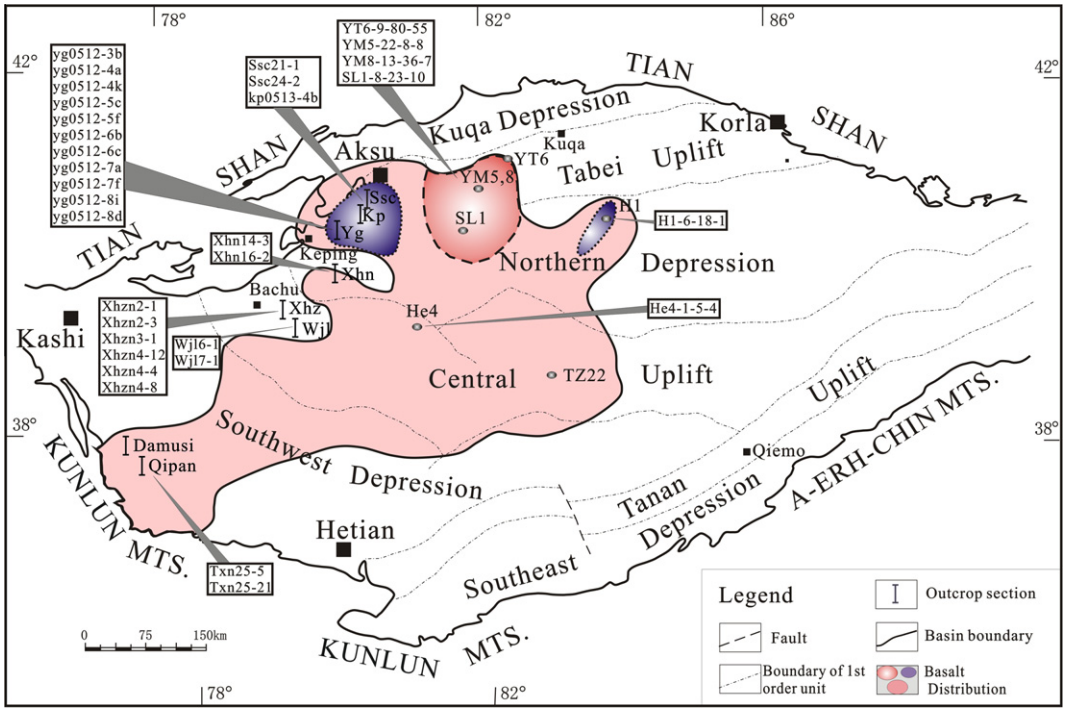

Fig. 1. A simplified tectonic map of the Tarim Basin, northwestern China, showing the distribution of Permian basalts in the Tarim Basin and the locations of some outcrops and drill holes sections with the samples in this study. The distribution of Permian basalts is after Yang et al. (2005), mainly based on available drill core data and outcrops in and around the basin.

Hf isotopic study on the TLIP is threefold: (1) to record the Hf isotopic signature of the TLIP rocks; (2) to determine the temporal Hf isotope variations in the TLIP rocks; and (3) to discuss the implications on the magma source of the basalts and intrusive rocks from the different areas of the Tarim Basin using the characteristics of Hf–Nd isotopes, as well as to make a comparison of Hf isotope signature in the TLIP rocks with that of the Siberia, Hawaii and Yellowstone volcanic rocks related with the CFB, mantle plumes and hotspots.

2. Regional geology and Permian igneous rocks in the Tarim Basin

The Permian magmatic event was as a large scale magmatic activity in the Tarim Basin (Yang et al., 2007a; Zhang et al., 2011). The TLIP is widely distributed in the Keping, Bachu, Tabei (northern Tarim Basin), Tazhong (central Tarim Basin) and Taxinan (southwestern Tarim Basin) areas (Fig. 1), and covers an area of ca. 250,000 km^2 (Yang et al., 2005; Chen et al., 2006), comparable to that of the Emeishan LIP in SW China (Chung and Jahn, 1995; Xu et al., 2001). Lithological units of the TLIP are mainly continental flood basalts and diabases as well as layered mafic–ultramafic intrusions, mica-olivine pyroxenite breccia pipes, diabases and ultramafic dykes, quartz syenites, quartz syenite porphyry and bimodal dykes (Yang et al., 1996; Chen et al., 1997; Jiang et al., 2004a,b; Yang et al., 2006a,b, 2007a,b; Zhang et al., 2008; Li et al., 2010; Li et al., 2011). Permian basalts in the Tarim Basin occur in the outcrops around the basin (Keping and Taxinan areas) and have also been identified from drilled cores within the basin (Jiang et al., 2004b, 2006; Yang et al., 2005, 2006a; Li et al., 2008; Yu et al., 2009, 2011). The basalts have been recognized in the Kupukuziman Formation in the lower part and the Kaipaizileike Formation in the upper part of the Early Permian (Jiang et al., 2006; Yu et al., 2011). Li et al. (2008) argued that the basalts exposed in the lower Permian Qipan Formation of the southwestern Tarim Basin have geochemical affinity with those from the Keping area. The data from the drill holes and 3D seismic cross-sections show a thickness of ca. 2.5 km for the basaltic sequence and a total volume of 75,000 km^3 (Zhou et al., 2009; Tian et al., 2010; Yu et al., 2011). The Permian magmatic event is also manifested in eastern Kazakhstan, Salair, west Mongolia and large regions to the north between the Siberian Craton and Altay orogenic belt (Pirajno et al., 2009; Ao et al., 2010; Xiao et al., 2010). Yu et al. (2011) obtained the ages of 289.5 ± 2.0 Ma and 288.0 ± 2.0 Ma by zircon SHRIMP U–Pb dating from basalts from the bottom of the Kupukuziman Formation and the top of the Kaipaizileike Formation in the Yingan section in Keping area, probably indicating the onset and the culmination of the eruptions.

The intrusive rocks from the Bachu area (including Xiaohaizi and Wajilitag) include diabases, layered mafic–ultramafic intrusions, mica-olivine pyroxenite breccia pipes and ultramafic dykes, quartz syenites, and quartz syenite porphyry. Yang et al. (2006b, 2007a) documented that the Permian Xiaohaizi syenite and dikes are well-developed in the Xiaohaizi area in Bachu County of the northwestern Tarim Basin. Field occurrence of dykes in Bachu area of NW Tarim Basin shows that the dyke association is well developed with diabases, ultramafic rocks, and quartz syenitic dykes and that the syenite batholith intruded into the Silurian, Devonian, and Carboniferous-Lower Permian strata. The majority of the dykes show NW–NNW trend with vertical dips and formed during the Early Permian. In one of the outcrops, a purple quartz syenitic porphyry dyke with an approximately 1–2 m width occurs in direct contact with a dark-bluish diabase dyke in the Shuigongtuan area. The diabase dyke swarms in the western Tarim Basin intruded into the pre-Permian sedimentary strata. The ages for the layered intrusive rocks and syenitic rocks of ca. 274–284 Ma were obtained by whole-rock $^{40}Ar/^{39}Ar$ and zircon SHRIMP age dating (Yang et al., 1996, 2007a; Zhang et al., 2008; Li et al., 2011), and are regarded to have formed during the Early Permian. The age data indicate that the eruption of the basalts in the Tarim Basin generally occurred prior to the emplacement of the intrusive suite. Li et al. (2011) argued that the sequence of magmatism of the TLIP in the central and western parts of the Tarim Basin are basaltic lavas in the Kupukuziman and Kaipaizileike Formations (285–290 Ma), layered mafic–ultramafic intrusion, mica-olivine pyroxenite breccia pipes, diabase and ultramafic dyke, quartz syenite, quartz syenite porphyry and bimodal dyke (274–284 Ma).

3. Sample description

The samples analyzed were collected from five field sections of the Yingan, Sishichang, Xiahenan, Wajilitag, and Xiaohaizi areas, and the drill holes of He4, H1, YT6, SL1, YM5 and YM8 (Fig. 1, Table 1). In addition to the surface exposures of the flood-volcanics, several boreholes drilled for oil and gas exploration have sampled basaltic rocks at the depths of 810–5900 m in the central and northern parts of the Tarim Basin.

The various units of basaltic rocks identified are coeval and chemically similar (Li et al., 2008; Tian et al., 2010; Li et al., 2012). Their geological features are given in Jia (1997), Zhang et al. (2003), Yang et al. (2005) and Li et al. (2008). In general, the basalts have been classified into various compositional groups. The Group 1 (a, b) basalts are aphyric and locally hyaloclastitic, occasionally vesicular/amygdaloidal, and sometimes with rare phenocrysts of plagioclase (<3%). They show interlayering of porphyritic and aphyric varieties. The groundmass is composed of plagioclase (30–50%), basaltic glass (30–45%) and Fe–Ti oxides (5–10%). The basalts belonging to compositional Group 2 basalts are augite- (1–2%) and plagioclase (<2%)-phyric, with minor olivine, and occasional lavas are aphyric with rounded vesicles. Some lavas are more strongly porphyritic, with 2–10% plagioclase phenocrysts and sparse phenocrysts of olivine (1–2%) and augite (1–3%). Groundmass textures vary from interstitial, through microlitic, to devitrified glassy, and the crystalline groundmasses are typically composed of plagioclase (30–45%), clinopyroxene (30–45%), olivine (<45%) and Fe–Ti oxides (5–10%). The magmatic stratigraphy of the Yingan section of Keping area was described in detail in Yu et al. (2011) and YQ Li et al. (2012). The Yingan section in the Keping County (Fig. 1) is one of the best Permian basalt outcrops in the study area and was hence selected for Hf-isotopic investigation in this study. The stratigraphy and geochemistry, including PGE were described by Yu et al. (2011) and YQ Li et al. (2012), where the eight basaltic lava flow units of a total thickness of ca. 400 m were recorded. Among these, the 2 units are exposed in the Kupukuziman Formation and 6 units in the Kaipaizileike Formation. Individual basaltic unit ranges from 10 to 70 m in thickness, with intercalations of terrestrial sediments such as alternating reddish mudstone and siltstone, volcanic breccia, tuff and non-marine limestone (Yu et al., 2011). A total of 32 representative samples were selected from more than 120 samples collected. The samples were analyzed for major, trace and rare earth elements as well as Sr–Nd–Pb isotopes, followed by Hf isotope study. Among these, 2–3 basalt samples were collected from individual lava flow units in the Group 1a basalts of the Yingan section to evaluate the Hf isotope variations among the individual units. The basalts from the middle and upper parts of the 5th unit is exceptional in that they carry abundant plagioclase phenocrysts (ca. 40 modal%).

The olivine-pyroxenite and diabase near the southern part of the Xiaohaizi reservoir in Bachu area occur as dykes intruding

Table 1
Hf isotopes and related chemical data of the TLIP rocks.

Rock types	Samples	Rock name	$^{176}Hf/^{177}Hf$	2σ	Hf_i	$\varepsilon Hf(t)$	SiO_2	FeO_T	MgO	Mg#	εNd	$^{87}Sr/^{86}Sr_i$
	Txn25-5	Basalt	0.282664	0.000010	0.282659	−3.4	46.29	15.02	4.46	34.6	−2.83	0.7074
	Txn25-21	Basalt	0.282630	0.000009	0.282625	−4.7	46.56	15.28	3.91	31.3	−2.81	0.7070
	Xhn14-3	Basalt	0.282584	0.000010	0.282580	−6.2	47.42	12.14	2.75	28.8	−3.85	0.7081
	Xhn16-2	Basalt	0.282621	0.000007	0.282615	−5.0	46.61	15.57	5.03	36.5	−3.37	0.7076
	yg0512-3b	Basalt	0.282710	0.000009	0.282705	−1.8	46.43	14.81	6.57	–	–	–
	yg0512-4a	Basalt	0.282723	0.000010	0.282718	−1.4	44.82	12.93	3.84	–	−2.28	0.7075
	kp0513-4b	Andesitic basalt	0.282637	0.000009	0.282632	−4.4	48.02	12.35	2.42	25.9	−2.88	0.7065
	yg0512-4 k	Basalt	0.282696	0.000009	0.282691	−2.3	45.85	15.21	5.72	–	−2.07	0.7062
Group 1a basalt	yg0512-5c	Basalt	0.282606	0.000008	0.282601	−5.5	47.51	15.09	5.39	–	−3.59	0.7069
	yg0512-5f	Basalt	0.282678	0.000012	0.282673	−2.9	46.37	15.59	6.15	41.3	−3.04	0.7067
	yg0512-6b	Basalt	0.282653	0.000008	0.282648	−3.8	46.27	15.63	5.14	37.0	−4.16	0.7068
	yg0512-6c	Basalt	0.282679	0.000010	0.282675	−2.9	46.01	15.98	6.08	40.4	−3.22	0.7067
	yg0512-7a	Basalt	0.282644	0.000007	0.282639	−4.1	43.39	18.47	5.48	34.6	−2.60	0.7067
	yg0512-7f	Basalt	0.282665	0.000007	0.282660	−3.4	43.62	18.30	3.28	24.2	−3.00	0.7070
	yg0512-8i	Basalt	0.282672	0.000008	0.282667	−3.2	45.76	15.40	6.35	42.4	−2.64	0.7065
	yg0512-8d	Basalt	0.282593	0.000009	0.282589	−5.9	47.01	17.55	3.63	26.9	−4.09	0.7077
	He4-1-5-4	Basalt	0.282684	0.000015	0.282679	−2.8	48.85	15.77	4.07	31.5	−5.17	0.7081
	Ssc21-1	Basalt	0.282634	0.000008	0.282628	−4.5	51.71	14.64	3.40	29.3	−4.14	0.7083
Group 1b basalt	Ssc24-2	Basalt	0.282611	0.000010	0.282606	−5.3	52.36	14.72	3.42	29.3	−4.07	0.7083
	H1-6-18-1	Basalt	0.282658	0.000007	0.282653	−3.7	50.16	15.47	3.15	26.6	−3.47	0.7076
	YT6-9-80-55	Basalt	0.282684	0.000008	0.282681	−2.7	48.33	13.53	7.96	51.2	−0.15	0.7051
Group 2 basalt	YM5-22-8-8	Basalt	0.282665	0.000011	0.282661	−3.4	52.49	11.22	5.96	48.6	−1.36	0.7050
	YM8-13-36-7	Basalt	0.282649	0.000011	0.282646	−3.9	53.71	9.32	3.77	41.9	−1.33	0.7053
	SL1-8-23-10	Basalt	0.282662	0.000009	0.282659	−3.5	55.13	9.91	6.62	54.4	−1.22	0.7053
	Xhzn2-1	Ol pyroxenite	0.282789	0.000021	0.282785	1.0	42.22	15.68	19.87	69.3	2.29	0.7043
	Xhzn2-3	Ol pyroxenite	0.282776	0.000016	0.282772	0.5	40.88	17.41	21.77	69.0	2.15	0.7040
	Wjl6-1	Pyroxenite	0.282729	0.000010	0.282728	−1.0	37.96	19.00	11.17	–	1.66	0.7051
	Wjl7-1	Diabase	0.282765	0.000009	0.282763	0.2	43.65	9.82	3.29	–	3.66	0.7036
Intrusive rocks	Xhzn3-1	Diabase	0.282621	0.000010	0.282617	−4.9	51.98	11.31	3.71	36.9	−2.36	0.7061
	Xhzn4-12	Diabase	0.282733	0.000009	0.282729	−1.0	46.10	13.90	4.93	38.7	2.64	0.7042
	Xhzn4-4	Syenitic porphyry	0.282788	0.000007	0.282785	1.0	67.08	3.56	0.38	16.0	–	–
	Xhzn4-8	Syenitic porphyry	0.282837	0.000006	0.282835	2.8	67.54	3.84	0.46	17.6	–	–

Note: ε values calculated using CHUR (today) with $^{143}Nd/^{144}Nd = 0.512647$; $^{147}Sm/^{144}Nd = 0.1967$. $\varepsilon Nd(t)$ and $\varepsilon Hf(t)$ being calculated at $t = 289$ Ma and $t = 275$ Ma for the basalts and intrusives, respectively. σ = Standard error of the mean and Mg# = $Mg/(Mg + Fe^{2+})$. The $^{176}Hf/^{177}Hf$ being from this study, and SiO_2, FeO, and MgO and Sr–Nd isotope values of basalts are from Li et al. (2008), Yu et al. (2011), ZL Li et al. (2012) and of intrusive rocks from Yang et al. (2006a,b, 2007a,b) and authors' unpublished data. Nd isotope data not reported in this paper. Ol: olivine, Hf_i: initial Hf.

the Carboniferous sedimentary rocks, which the latter underwent contact metamorphic effect (sample locations described in Yang et al., 2007a,b). The diabase dykes intruded into the Devonian to Silurian sedimentary sequences in the Xiaohaizi and Wajilitag areas in Bachu area, and have similar mineral assemblages and textures with those of the Keping basalts. The petrographic and geochemical features of these rocks are reported in Yang et al. (2007a), Zhang et al. (2008) and Li et al. (2011). The ages of these rocks are estimated as ca. 275 Ma, younger than those of the basalts described above. The Wajilitag mafic–ultramafic complex, located in Bachu area of the Tarim Basin, mainly includes olivine pyroxenite, pyroxenite and gabbro and diabase, and hosts Fe–Ti mineralization. The sequence of crystallization as inferred from mineral paragenesis is: olivine, clinopyroxene, magnetite and ilmenite.

4. Geochemical characteristics of the Tarim Permian basalts and intrusive rocks

4.1. Tarim Permian basalts

In general, the TLIP basalts show SiO_2 contents from 43.7 to 53.6 wt.%, with K_2O contents always lower than Na_2O. The basalts belong to both alkaline and subalkaline series. All the basalts are rather evolved (100 Mg# from 22.3 to 59.3), and most of them show high TiO_2 contents (mainly 3–5 wt.%), classifying as high-Ti series basalts. According to the classification by ZL Li et al. (2012), three compositional groups have been identified for the TLIP basalts as defined from their HFSE and P_2O_5 contents. The Groups 1 and 2 basalts are clearly differentiated on the basis of their different Nb/Y values, with two subgroups (Group 1a, Group 1b) identified within the Group 1 basalts, based on their distinct P_2O_5 vs. Mg# trends and P_2O_5/Ce ranges (not shown here). The Group 1 basalts include alkaline and moderately subalkaline rocks and have distinctly lower SiO_2 and generally lower K_2O, and higher FeO_T, TiO_2, P_2O_5 than those of the Group 2 lavas. The Group 1 basalts are from the field sections of Yingan, Sishichang, and Taxinan, and the drill holes of TZ22, He4, and H1; whereas the Group 2 basalts span the alkaline and subalkaline series, and come from the SL1, YT6, YM5 and YM8 drill holes (Fig. 1). All the basalts are strongly enriched in LILE and LREE, have high LREE/HREE, no Eu anomalies and no Nb–Ta anomalies. The chondrite-normalized REE patterns of both the groups show LREE-enrichment, with moderate HREE depletion ($(Gd/Lu)_N$ of 1.7–3.3) and their Eu/Eu^* ratios show a limited range (0.8–1.1), indicating only weak or no Eu anomaly. The Group 2 basalts show slightly steeper LREE-enrichment and more HREE depletion than the Group 1 basalts, although there is effectively no significant difference in REE patterns between the two sub-groups despite their markedly different P_2O_5/Ce values. A more detailed description of the geochemical features of the three groups of basalts is given in ZL Li et al. (2012).

4.2. Tarim Permian intrusive rocks

The olivine-pyroxenite with an average abundance of SiO_2 around 42%, 100 Mg# = 67–69 was probably derived from a primary basaltic magma rich in iron and magnesium, with significant fractionation as suggested by the enrichment of the marked slope from LREE to HREE. These rocks show geochemical features similar to those of within-plate basalts, with LREE enrichment and lack of

Eu anomaly. Their trace elements ratios suggest a potential magma source from the mantle. It is possible that the magma was derived from partial melting of asthenospheric mantle, and intruded along fractures in the basement rocks (Yang et al., 2007b). The diabase dykes which occur in close proximity to the olivine pyroxenite dyke, show geochemical characteristics broadly similar to those of the Keping basalts suggesting that they might have been derived from a similar magma source in the same within-plate setting. Yang et al. (2007a) showed that the geochemistry of the quartz syenite porphyry in Bachu Shuigongtuan indicates A-type affinity, formed under within-plate rifting environment and derived from mantle sources at ca. 277 Ma, and probably representing the last major magmatic event in the Tarim Basin. The quartz syenite porphyry has almost the same geochemical features with the Xiaohaizi syenite, and both of them show similar source characteristics and tectonic setting. The chemical characteristics of the diabase indicate derivation from mantle source and formation under within-plate environment, with probable affinity with mantle plumes. The formation of the quartz syenite porphyry and diabase are genetically linked with the voluminous Permian (285–290 Ma) basalts occurring in the Tarim Basin.

5. Analytical methods

The 32 whole-rock samples selected for this study were crashed by jaw crusher and roller mill, and then powdered in agate mortars in order to minimize potential contamination of transitional metals. The amygdules in some basalt samples were carefully removed as best as possible to minimize the effect of post-eruption hydrothermal alteration.

Hf isotopes were determined using a Finnigan Neptune multi collector (MC)-ICP-MS at the Guangzhou Institute of Geochemistry of Chinese Academy of Sciences. The measured $^{176}Hf/^{177}Hf$ ratios were normalized to $^{179}Hf/^{177}Hf = 0.7325$, and the reported $^{176}Hf/^{177}Hf$ ratios were further adjusted relative to the JB-3 standard of 0.282160. The analytical procedures used are similar to those described by Li et al. (2005, 2007). The Hf isotopic results are listed in Table 1. The $\varepsilon Hf(t)$ values were calculated with reference to the chondritic reservoir (CHUR) with present-day $^{176}Hf/^{177}Hf = 0.282772$ and $^{176}Lu/^{177}Hf = 0.0332$ (Blichert-Toft and Albarède, 1997).

6. Analytical results

The $^{176}Hf/^{177}Hf$ isotopic ratios of the basalt samples range from 0.282584 to 0.282837. The Group 1a, Group 1b, and Group 2 basalts have $^{176}Hf/^{177}Hf$ ratios of 0.282584–0.282723, 0.282611–0.282658, and 0.282649–0.282684, respectively (Table 1). The pyroxenites, diabases, and felsic dykes show $^{176}Hf/^{177}Hf$ ratios of 0.282789–0.282776, 0.282765–0.282621, and 0.282785–0.282835, respectively. The $\varepsilon Hf(t)$ in the Group 1a, Group 1b and Group 2 basalts are -0.4–4.4, 0.5–2.1, and 1.9–3.1, respectively, and the intrusive olivine pyroxenite, diabase and syenitic porphyry show 6.0–6.5, 4.5–5.7 (except the value of 0.6 for a sample of diabase), and 6.5–8.3, respectively.

7. Discussion

7.1. Spatial and temporal comparison of Hf isotopic systems from the three group basalts and intrusive rocks

As summarized in a previous section, the Tarim basalts show an age range of 285–290 Ma. The results from present study show that the Hf isotopes ($^{176}Hf/^{177}Hf$ and $\varepsilon Hf(t)$) of the three groups basalts (Group 1a, Group 1b and Group 2) do not display any marked contrast. However, the $\varepsilon Hf(t)$ of the Group 1a rocks show a much wider range, and overlap with the ranges of the Group 1b and Group 2 rocks. The Txn basalts from the southwestern Tarim Basin show almost the same Hf isotope features to those from Keping area (Yg, Ssc). The Hf data combined with trace elements and Sr–Nd–Pb isotopes, suggest that these basalts may be derived from the same OIB-like magmatic sources, but underwent evolved magmatic processes in some extent. In the Yingan section, there is a discontinuous change of the trace element ratios and Sr–Nd isotopes from the bottom unit to the top unit of the basalts, suggesting probable a mixing process between the evolved magma and a relatively primitive magma source (YQ Li et al., 2012). Hf isotopes of the basalts from the Yingan section show variation from 0.282644 to 0.282679 at the top of the Kai2 unit to the bottom of the Kai3 unit, from 0.282653 to 0.282678 from the top of the Kai3 to Kai4, and from 0.282696 to 0.282637 from the top of the Kai4 to the bottom of the Kai5 unit. Variation also exists within individual units, such as an increase in Hf isotope from 0.282593 to 0.282672 in Kai1 and from 0.282696 to 0.282723 in Kai5 (from the bottom to the top). The Hf isotope variation from the bottom unit to the top unit as recorded in the present study shows an abrupt and pronounced change from the beginning of the unit Kai1 till Kai6, with the exception of the Kai2 unit (Fig. 4b).

However, the intrusive units formed during 274–284 Ma, and are much younger than the basalts (Li et al., 2011). The intrusive suite show much higher $^{176}Hf/^{177}Hf$ and $\varepsilon Hf(t)$ values than the three groups of basalts (Fig. 2 and 3), indicating that they may be derived from a different componental proportion of magma sources. Furthermore, the $\varepsilon Hf(t)$ in the olivine pyroxenite is relatively higher than the diabase, and the syenitic porphyry has the highest $\varepsilon Hf(t)$ values compared to those from the basalts and olivine pyroxenite and diabase although they are plotted in similar or the same field with relatively high $\varepsilon Nd(t)$ and $\varepsilon Hf(t)$ among the various units in the Tarim LIP. The mafic intrusive rocks (olivine pyroxenite and diabase) and the syenite porphyry have the similar age between 274 Ma and 284 Ma, and have genetic affinity in the sources and magmatic evolution as described by Zhang et al. (2008). Zhang et al. (2008) argued that the Bachu layered igneous complex including mafic rocks and syenite were derived from mantle source by crystal fractionation and accumulation, and is similar to those of many oceanic and continental alkaline primary suites having positive $\varepsilon Nd(t)$ in association with LREE enrichments relative to Normal-MORB-mantle-derived rocks (N-MORB; Wedepohl and Baumann, 1999). In this context, the high $\varepsilon Nd(t)$ and

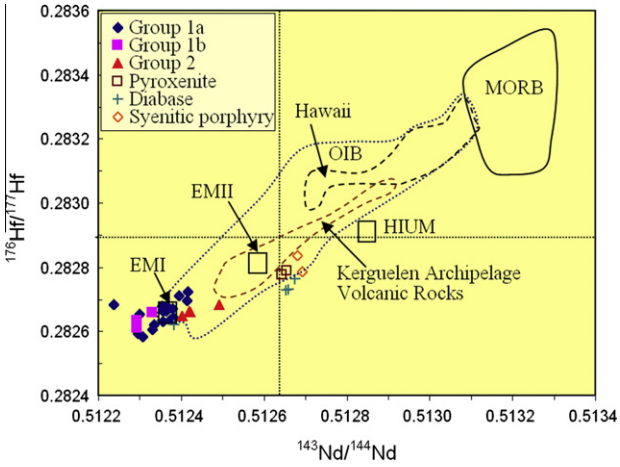

Fig. 2. $^{176}Hf/^{177}Hf$–$^{143}Nd/^{144}Nd$ diagram for the TLIP rocks. The fields for OIB and MORB being from Salters and Hart (1991).

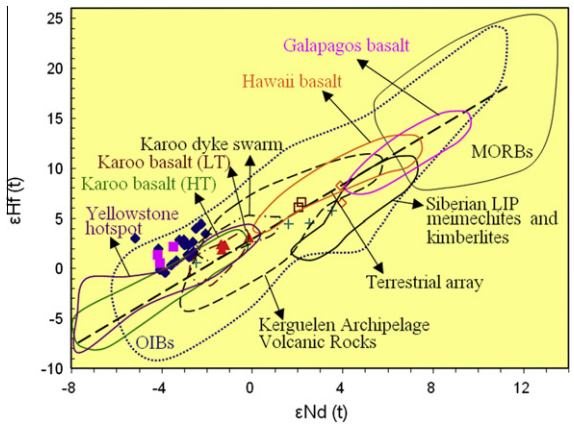

Fig. 3. $\varepsilon Hf(t)$-$\varepsilon Nd(t)$ diagram for the TLIP rocks. HT: high-Ti; and LT: low-Ti. The fields for the Hawaii basalt (Blichert-Toft et al., 1999), Karoo basalt (HT, LT) and swarm dykes (Ellam, 2006; Jourdan et al., 2007); Siberian meimechites and kimberlites (Carlson et al., 2006); Yellowstone hotspot tuffs (Nash et al., 2006); Galapagos Islands (Blichert-Toft and White, 2001); and Kerguelen Archipelage volcanic rocks (Mattielli et al., 2002). The regression line of the terrestrial array being from Vervoort et al. (1999). The fields for the OIB and MORB being from Patchett and Tatsumoto (1980), Patchett (1983a), Salters and Hart (1991), Salters (1996), Nowell et al. (1998), Salters and White (1998), Blichert-Toft and Albarède (1999), Blichert-Toft et al. (1999), and Chauvel and Blichert-Toft (2001).

$\varepsilon Hf(t)$ in them further support Zhang et al. (2008)'s argument in the present study.

Combined with the previous major, trace and Sr–Nd isotope study, the Taxinan basalts show similar geochemical and Sr–Nd isotope characteristics, and are regarded to have been derived from the same magma source and/or varied magmatic evolution. The Hf isotope data presented in this study support the assumption that the Taxinan basalt belongs to the Group 1a basalts being from the same magma source and witnesses similar magmatic processes with those of the Keping basalts (Yg and Ssc and Xhn basalts), constituting a flood basaltic province in the Tarim Basin during the Early Permian.

With regard to the spatial and temporal distribution of Hf isotopes in the Tarim Basin, the intrusive rocks in the Bachu area formed during the age of 274–284 Ma show higher $^{176}Hf/^{177}Hf$ and $\varepsilon Hf(t)$ values. Moderate $^{176}Hf/^{177}Hf$ and $\varepsilon Hf(t)$ values are observed for the basalts in the Keping, Taxinan and Tabei areas formed during the age of 285–290 Ma. The He4 drill hole sample belonging to the Group 1a basalts shows the lowest $\varepsilon Nd(t)$ value among the various units in the Tarim basalts, although the $\varepsilon Hf(t)$ values of these rocks are within the range of the Group 1a basalts.

7.2. Implication for magma source

The TLIP basalts have low $\varepsilon Nd(t)$ and moderate $\varepsilon Hf(t)$ ratios, indicating a low $\varepsilon Nd(t)$ and moderate $\varepsilon Hf(t)$ OIB-like source. As seen in Fig. 2, the majority of the OIB data fall in a tight array that encompasses the EMI end member (Walvis Ridge, Pitcairn) at the low $^{176}Hf/^{177}Hf$ end of the array, and the EMII end member comparable to those of Iceland, Hawaii, Ascension, New Amsterdam and St. Paul define the high $^{176}Hf/^{177}Hf$ end of the array (Salters and White, 1998). The samples of the TLIP basalts generally show a good positive correlation between $^{176}Hf/^{177}Hf$–$^{143}Nd/^{144}Nd$, and fall in the field of OIB with low $^{176}Hf/^{177}Hf$ and $^{143}Nd/^{144}Nd$ except for a sample from the He4 which has the lowest $\varepsilon Nd(t)$ and medium–high $\varepsilon Hf(t)$ values (Fig. 2). The TLIP basalts have comparable $^{176}Hf/^{177}Hf$ (0.28258–0.28284) and $^{143}Nd/^{144}Nd$ ratios (0.512237–0.512502) with those from the basaltic lavas ($^{176}Hf/^{177}Hf$ of 0.28265–0.28278, $^{143}Nd/^{144}Nd$ of 0.512439–0.512545) of the Pitcairn hotspot (Woodhead and McCulloch, 1989). The low $^{176}Hf/^{177}Hf$, $^{143}Nd/^{144}Nd$ and $^{206}Pb/^{204}Pb$ of the Tarim basalts correspond to an enriched signature resulting by the incorporation of partial melts of enriched lithosphere mantle source in the early stages of the plume activity.

The Group 1a basalts have lower $\varepsilon Hf(t)$ and $\varepsilon Nd(t)$ values concentrated in the field of OIB end member with low $\varepsilon Hf(t)$ and $\varepsilon Nd(t)$ (Fig. 3). The Group 1b basalts plot along the Hf–Nd array of the Group 1a basalts. The Group 2 basalts have much higher $\varepsilon Nd(t)$ than those from the Group 1a basalts, defining a separate Hf–Nd array. However, pyroxenite, diabase and syenitic porphyry plot in the field of higher $\varepsilon Nd(t)$ and $\varepsilon Hf(t)$, close to EMII end member, but with much higher $\varepsilon Nd(t)$. Both the $\varepsilon Hf(t)$ and $\varepsilon Nd(t)$ values from the Group 1a, Group 1b and Group 2 basalts and intrusive rocks fall in the different fields of the OIB. Therefore, the Hf combined with Nd isotopic characteristics presented here might reflect the nature of the mantle beneath Tarim and the overlapping isotopic compositions comparable to those observed in intraplate OIB (Figs. 2 and 3).

Our new Hf isotopic data may provide important clues to evaluate the differences between the basalts (285–290 Ma) and the intrusive rocks (274–284 Ma) (Fig. 3). In the $\varepsilon Hf(t)$ vs. $\varepsilon Nd(t)$ plot, the en-echelon arrays for the Tarim basalts and intrusive rocks might correspond to two different periods of magmatic activity and evolved magmatic process in the Tarim Basin during Early

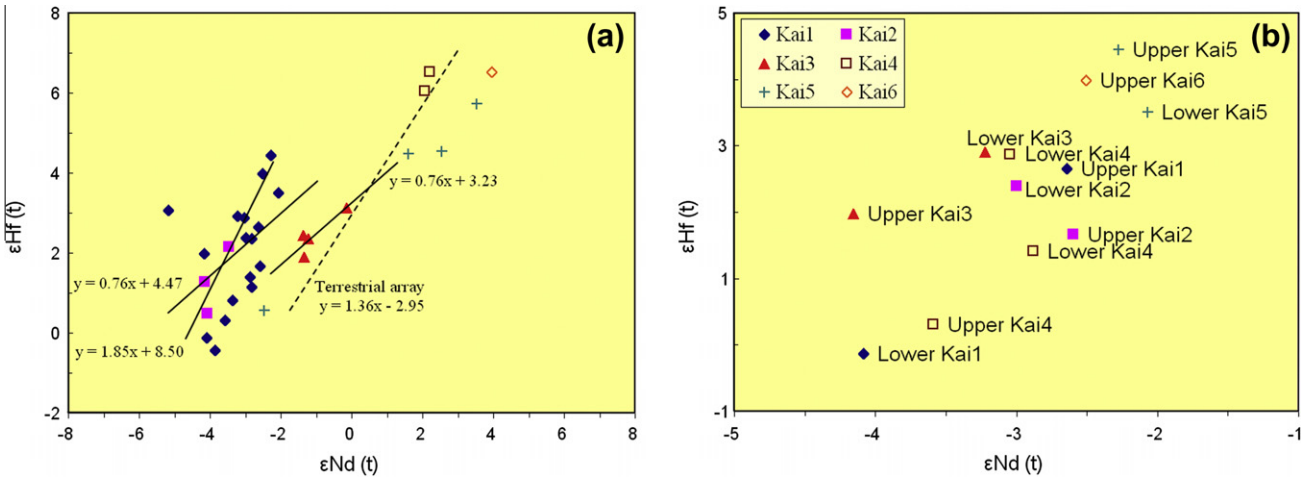

Fig. 4. (a) $\varepsilon Hf(t)$–$\varepsilon Nd(t)$ diagram for the intercepts and slopes of the TLIP rocks, and (b) $\varepsilon Hf(t)$–$\varepsilon Nd(t)$ diagram for the Ka1–Kai6 unit basalts from the Yg section.

Permian. Furthermore, the intrusive rocks show much more affinity with the Group 2 basalts in the Hf–Nd array (Fig. 3), indicating that their source characteristics and evolutionary history are much closer to those of the Group 2 basalts. Taken together, the $\varepsilon Hf(t)$–$\varepsilon Nd(t)$ isotopic array for the basalts (except for sample He4-1-5-4) and intrusive rocks (pyroxenite and diabase, except for syenitic porphyry) define a linear array with the intercept I of 3.89 and 3.17 and the slope S of 0.68 and 0.93 respectively (Fig. 4a). The array is characterized by low-angle and slightly shallower slopes than those of the global mantle array (1.33, not shown here) and the terrestrial array (1.36) (Vervoort et al., 1999). Furthermore, the Group 1b basalts show slightly steeper distribution (an intercept I of +8.5 and a slope S of +1.85) than the slopes of the terrestrial array. However, the Group 1a and Group 2 basalts show intercepts at 4.47 and 3.23 with a similar slope of 0.76, being much gentler than that of the terrestrial array. Individual oceanic island arrays (Salters and White, 1998; Blichert-Toft et al., 1999; Kempton et al., 2000) are commonly characterized by shallower slopes (e.g. Pitcairn Island and Hawaiian basalts, $S \sim 1.00$, Eisele et al., 2002), whereas the arrays for Walvis Ridge, another EMI-type locality, and Iceland (Kempton et al., 2000), have steeper slopes ($S > 1.5$). The slope of the $\varepsilon Hf(t)$-$\varepsilon Nd(t)$ isotopic array and source components from the TLIP Group 1a and Group 1b basalts can be comparable to the Karoo CFB basalt (HT), although the former has a much higher $\varepsilon Hf(t)$. The TLIP ultramafic–mafic intrusive rocks can be compared to the Siberian LIP meimechite and kimberlite, and Kerguelen Archipelago volcanic rocks. A sample from the drill hole of the He4 with lower $\varepsilon Nd(t)$ has distinct $\varepsilon Hf(t)$ and $\varepsilon Nd(t)$ values as compared to the other samples, with a good correlation between the $\varepsilon Hf(t)$ and $\varepsilon Nd(t)$, indicating the He4 rock was derived from a source distinct from that of other Group 1a basalts. However, such a distinction does not exist in the Sr–Nd relations, and the He4 sample coincides with the Group 1a basalts in $^{147}Nd/^{146}Nd$ vs. $^{87}Sr/^{86}Sr$ plot (not shown). However, the TLIP Group 2 basalts are similar to those of the Karoo CFB basalt (LT) and Karoo CFB Dyke swarm and Kerguelen Archipelago volcanic rocks. There is no systematic trend and correlation between the Hf isotopes and alkalinity index ($AI = (Na_2O + K_2O) - (0.37SiO_2 - 14.43)$; Rhodes, 1996). However, the high $\varepsilon Hf(t)$ from the olivine pyroxenite show subalkaline feature, whereas the low $\varepsilon Hf(t)$ from the Group 1a basalts (except for the He sample) and diabase are dominantly alkalic. The Group 1b and Group 2 basalts are tholeiitic and subordinately alkali. Furthermore, in the $\varepsilon Hf(t)$–$\varepsilon Nd(t)$ plot, the syenitic porphyry components are different compared to those from the felsic tuffs from the Yellowstone hotspots, with the former having higher $\varepsilon Hf(t)$ and $\varepsilon Nd(t)$ values (Fig. 3).

The possibility that the Tarim basalts were derived from enriched lithosphere mantle and OIB-like asthenophere mantle source is suggested from the Hf–Sr–Nd isotope and geochemical characteristics. Based on trace element and Sr–Nd isotope chemistry, Yu et al. (2011) and Zhou et al. (2009) proposed that the Tarim basalts were derived from OIB-like mantle source with less continental crust contamination. The weak Nb anomaly and the nearly chondritic Hf/Sm ratios (0.7 ± 0.1) preclude the possibility of significant contribution from continental crust material.

According to the highest Fo values (85) of olivine from the ultramafic dykes at the Bachu area, the liquidus temperature of olivine was as high as 1303 °C, and the corresponding liquidus temperature of the basaltic melts was 1200 °C ($K_D = 0.30 \pm 0.03$); and such high-Mg parental magmas with a high temperature further suggest that the magmas were generated from an upwelling mantle plume (Zhou et al., 2009). To estimate the role of the Tarim plume, we use chemical signatures generated by the plume and its interaction with shallow lithosphere materials during the rising of the plume to the surface. Previous studies show some evidences from isotopes and geochemistry that the Tarim basalts have OIB-like components, which indicate that these basalts suffered different degrees of interaction between plume melts and the underlying lithospheric mantle (Li et al., 2008, 2012; Zhang et al., 2008; Zhou et al., 2009; Tian et al., 2010). An important tool in deciphering the interaction of the plume magmas with the lithospheric mantle and oceanic crust is the relationship between the uncontaminated isotopic ratios of the source magmas and their major element chemistry. However, it is not easy for CFB to remain uncontaminated. Also, the data so far reported from Tarim suggest a weak crustal contamination. The geochemical and isotopic data such as alkalinity, MgO and other major element contents of basaltic magmas can be used to deduce the degree of interaction between the plume mantle and overlying lithospheric mantle during melting and differentiation processes. Typically, variation in MgO contents results from shallow-level olivine fractionation, whereas variation in alkalinity results from changes in degree of melting in the lithosphere (Chen and Frey, 1985), depth of melting, or clinopyroxene fractionation in the deeper part of the suboceanic lithosphere (Mattielli et al., 2002). Correlation between isotopic ratios and major elements can yield information on the interaction of plume magmas with the lithosphere. Good correlations between $\varepsilon Hf(t)$ and major-element compositions (e.g., SiO_2, MgO, FeO_T) and arc-shaped distribution in the Lu/Hf vs. Hf/Yb plot (Fig. 5d) in the Group 1a, Group 1b and Group 2 basalts indicate that the Group 1a, 1b and 2 basalts were generated by partial melting of a two-component mantle source and partly mixing process (Fig. 5d) except for a sample from the He4 drill hole and another sample from the Yg section (yg0512-4a, andesitic basalt) which show different chemistry (Fig. 5, Table 2). Although a good correlation exists between $\varepsilon Hf(t)$ and SiO_2, the $\varepsilon Hf(t)$ does not show a good correlation with MgO and FeO_T in the Group 1a basalt. Here we argue that the good correlation between $\varepsilon Hf(t)$ and major elements might be a reflection of the interaction of the two-component mantle sources.

The Sr and Nd isotopic compositions of the basalts from the Keping area overlap with those of typical OIB previously studied by Jiang et al. (2004a) and Zhou et al. (2009). The Group 1a and Group 1b basalts have similar $^{87}Sr/^{86}Sr$ ratios and initial $^{87}Sr/^{86}Sr$ (Sr_i) values; however, Group 2 basalts have much lower $^{87}Sr/^{86}Sr$ ratios and Sr_i values than those from the Group 1a and Group 1b basalts. Zhou et al. (2009) argued that the Keping basalts are OIB-like, and proposed a genetic link with mantle plume. Therefore, combined with the previous data and our present results, we suggest that the basalts were derived from the same primary magmas of asthenosphere mantle or mantle plume and had an interaction with the lithosphere mantle during its rising, although they subsequently underwent different evolutionary processes. Hf and Nd isotopic compositions are well correlated in the Group 1a, Group 1b, and Group 2 basalt samples, and olivine pyroxenite and diabase with the data falling within the array observed for OIB, except for the syenitic porphyry samples. A diabase sample (sample Xhzn3-1) from Xiaohaizi of Bachu area fall in the field close to the Group 1a basalt (Figs. 2, 3) and could be explained through a genetic link between the basalts and diabases although they formed in different time. The other sample of the diabase shows positive $\varepsilon Nd(t)$ and falls in the similar field of the olivine pyroxenite but with a lower $\varepsilon Hf(t)$ than that of the olivine pyroxenite. The isotopic variability among different igneous rocks can reflect distinct magma source proportions, as these rocks are also characterized by low $^{143}Nd/^{144}Nd$ and $^{176}Hf/^{177}Hf$ values, and high $^{87}Sr/^{86}Sr$ ratios (Jiang et al., 2004b; Zhou et al., 2009 and Fig. 6b in this study). In general, according to the above study, the basalts and intrusive rocks from the TLIP might be derived from different componental proportion of magma sources with different degree of partial melting of lithospheric mantle while the magmas upwelling from the OIB-like asthenospheric mantle and/or plume mantle, and the magma process by mainly fractional crystallization and

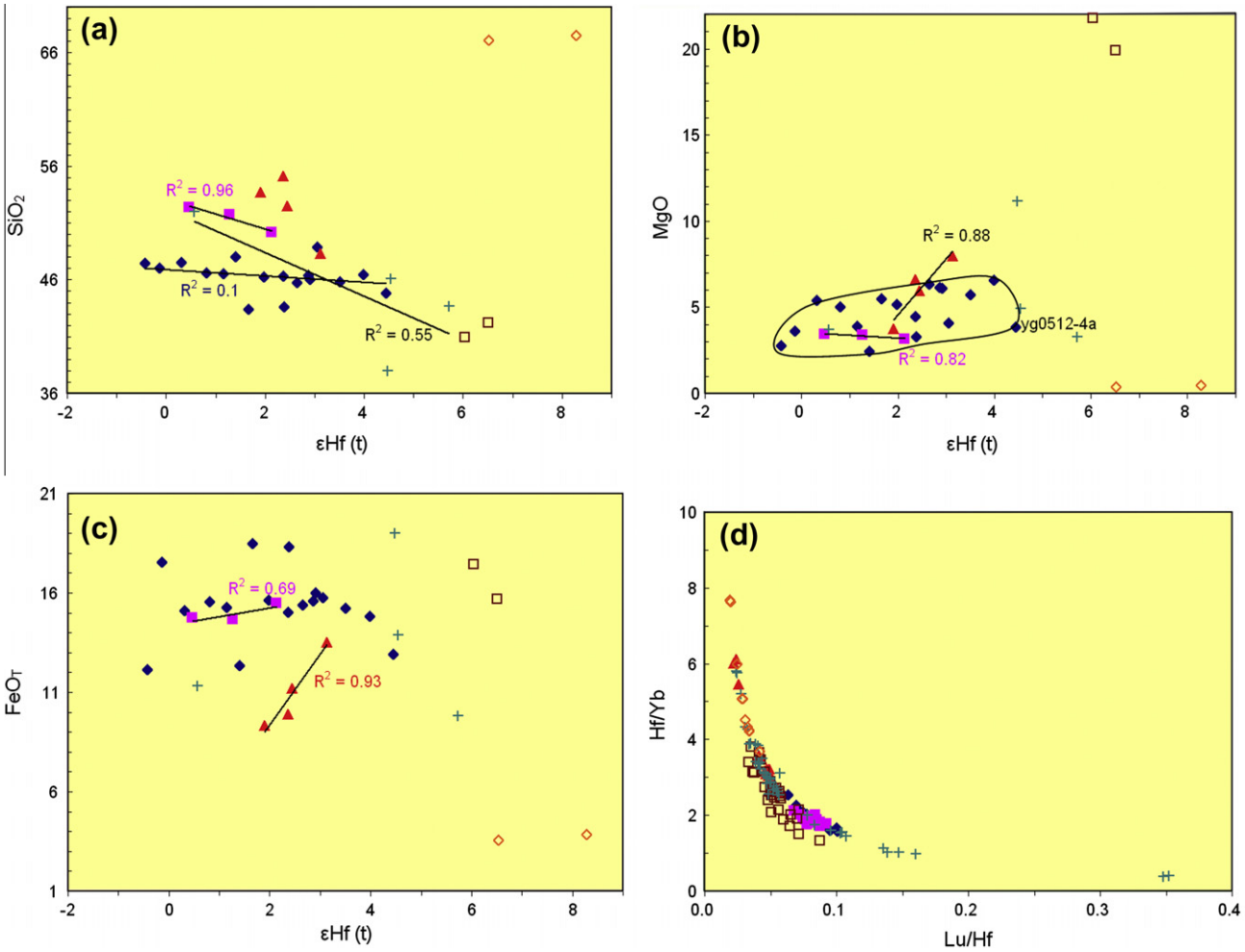

Fig. 5. (a) SiO_2-$\varepsilon Hf(t)$, (b) MgO-$\varepsilon Hf(t)$, and (c) FeO_T-$\varepsilon Hf(t)$ diagrams to show partial melting processes, and (d) Hf/Yb–Lu/Hf diagram for magmatic mixing process.

cumulation from the primary magma and/or OIB-like mantle source, respectively (Fig. 7).

Table 2
Sequences of the Ka1–Kai6 unit basalts from the Yg section.

Rock types	Samples	Rock name	Sequences
Group 1a basalt	yg0512–3b	Basalt	6th unit of the Kpz FM
	yg0512–4a	Basalt	Top of the 5th unit of the Kpz FM
	kp0513–4b	Andesitic basalt	Bottom of the 5th unit of the Kpz FM
	yg0512–4 k	Basalt	5th unit of the Kpz FM
	yg0512–5c	Basalt	4th unit of the Kpz FM
	yg0512–5f	Basalt	Bottom of the 4th unit of the Kpz FM
	yg0512–6b	Basalt	Top of the 3rd unit of the Kpz FM
	yg0512–6c	Basalt	3rd unit of the Kpz FM
	yg0512–7a	Basalt	Top of the 2nd unit of the Kpz FM
	yg0512–7f	Basalt	Bottom of the 2nd unit of the Kpz FM
	yg0512–8i	Basalt	Top of the 1st unit of the Kpz FM.
	yg0512–8d	Basalt	1st unit of the Kpz FM

Note: Kpz FM = Kaipaizileike Formation.

7.3. Magma evolution and comparison with other large igneous provinces in the world

As the majority of the flood basalts in the Tarim Basin were erupted at around 285–290 Ma (Li et al., 2011), based on the Hf isotopic features as well as the relatively homogenous character of the CFB and their widespread distribution, we suggest that the isotopic compositions of the Tarim Group 1a basalts are likely to reflect the mantle source composition of the main volume of the Tarim plume and might include less recycled oceanic crust and/or continental crust.

We selected $\varepsilon Hf(t)$ and $\varepsilon Nd(t)$ values of the Karoo CFB basalt (HT and LT), Karoo CFB dyke swarm, Siberian LIP meimechite and kimberlite, Yellowstone hotspot felsic tuff, Hawaii basalt, Galapagos basalt, Kerguelen Archipelago volcanic rocks, and SW Australia flood basalt for comparison. From Fig. 3, the Group 1a, Group 1b and Group 2 basalts fall in the end member of OIB with low $\varepsilon Hf(t)$ and $\varepsilon Nd(t)$ values close to the enriched mantle source. The $\varepsilon Hf(t)$ and $\varepsilon Nd(t)$ of the basalts are comparable to the Karoo CFB basalt (HT), Kerguelen Archipelago volcanic rocks and Yellowstone hotspot, and those of the intrusive rocks are similar to the Siberian LIP meimechite and kimberlite with mixing components of low $\varepsilon Hf(t)$-$\varepsilon Nd(t)$ and high $\varepsilon Hf(t)$ and $\varepsilon Nd(t)$ of the OIB. The Tarim Group 1a basalts have similar $\varepsilon Hf(t)$ and $^{206}Pb/^{204}Pb$ components (Fig. 6) compared to the high-Ti basalts from the Karoo CFB, particularly Karoo CFB picritic basalts (Ellam, 2006) with a relatively higher $\varepsilon Hf(t)$ and $^{206}Pb/^{204}Pb$. The Siberian LIP meimechite and

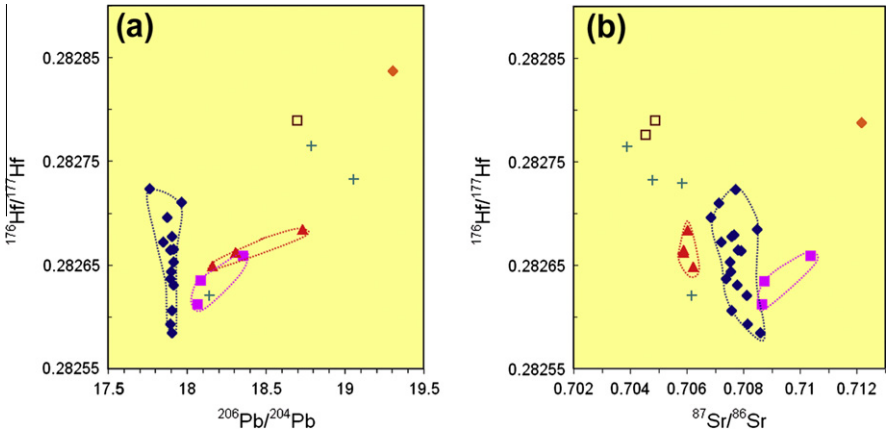

Fig. 6. (a) $^{206}/^{204}$Pb–^{176}Hf/^{177}Hf and (b) ^{87}Sr/^{86}Sr–^{176}Hf/^{177}Hf diagrams for the TLIP rocks. *Note*: the data of ^{206}Pb/^{204}Pb and ^{87}Sr/^{86}Sr being from authors' unpublished data.

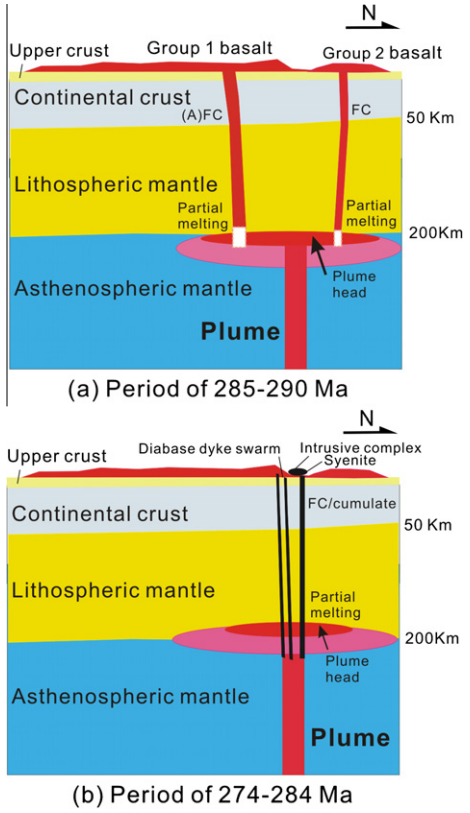

Fig. 7. A tectonic model for the formation of the basalts in (a), and intrusive rocks in (b) from the TLIP.

kimberlite have much higher εHf(t) and ^{206}Pb/^{204}Pb than those from the Tarim flood basalts. The low εNd(t) is distinct from that of MORB and OIB, and is therefore attributed to the continental plate (ZL Li et al., 2012), suggesting that an enriched subcontinental lithosphere mantle might be a source candidate for the formation of the Tarim basalts. The olivine pyroxenite, diabase and felsic rocks from the Tarim Basin might have been derived from different magma source/magma process compared to the basalts because they show much higher εHf(t), εNd(t) and ^{206}Pb/^{204}Pb than those from the Tarim basalt lavas. But we suggest that they may be derived from the similar magma sources and suffered evolved magmatic processes, such as the different evolved stages during the process of fractional crystallization after partial melting of mantle sources.

The Tarim flood basalts (including Groups 1a, 1b, and 2) have lower ^{143}Nd/^{144}Nd and higher ^{87}Sr/^{86}Sr values than the Xiaohaizi and Wajilitag ultramafic–mafic rocks (Zhang et al., 2008; Li et al., 2012a,b). This phenomenon is comparable to that in the Siberian Traps, where most of the flood basalts have lower ^{143}Nd/^{144}Nd and higher ^{87}Sr/^{86}Sr values than the high-MgO Maymecha-Kotuy samples (Lightfoot et al., 1990; Sharma et al., 1991; Wooden et al., 1993). The isotopic range of the Maymecha-Kotuy samples overlaps the isotopic variation seen in intraplate OIB. In the Tarim Basin, flood basalts also have much lower ^{143}Nd/^{144}Nd and higher ^{87}Sr/^{86}Sr values than the high-MgO olivine pyroxenite and diabase with same MgO (except for one sample of the diabase). The mafic intrusive rocks which show distinct geochemistry and isotopes, support the models proposed for the Siberian flood basalts and Maymecha-Kotuy samples (Carlson et al., 2006) with either a larger percentage of the pyroxene-rich component present in the Maymecha-Kotuy source, or crustal contamination of the basalts. We favor that the mafic intrusive rocks should be derived from an OIB-like asthenospheric (plume) mantle in an extensional regime by crystal cumulation and fractionation (with negligible crustal contamination) of alkali basalts using the data of trace elements and Sr–Nd isotope features in the Bachu layered intrusions by Zhang et al. (2008).

Clinopyroxene, amphibole and garnet exert major control on the fractionations of Lu/Hf and Sm/Nd values. For example, the fractionation of Lu/Hf and Sm/Nd controlled by clinopyroxene results in too low f(Lu/Hf)/f(Sm/Nd) values for shallow level melting (Salters and Hart, 1991). Garnet and amphibole are the two most obvious phases that can affect f(Lu/Hf)/f(Sm/Nd). Although amphibole does fractionate Lu/Hf more than clinopyroxene, there is a concomitant change in Sm/Nd fractionation (Salters and Hart, 1991). Garnet is able to fractionate Lu/Hf more significantly and melting in the presence of garnet will result in higher f(Lu/Hf)/f(Sm/Nd) values. Only modest amounts of garnet (modal garnet-clinopyroxene ratios of 0.15–0.25) are required to result in the appropriate f(Lu/Hf)/f(Sm/Nd) values and will explain the slope of the OIB array (Salters and White, 1998). Based on these studies, we presume that the higher f(Lu/Hf)/f(Sm/Nd) values and the εHf(t)/εNd(t) values in the Tarim Group 1a and Group 1b basalts are mainly controlled by garnet, and not by clinopyroxene and amphibole. However, in the Tarim Group 2 basalts, clinopyroxene fractionation is significant. Alternatively, the low end of the OIB array can also be explained by the recycling of a fixed mixture of sediment and ancient basalt as described by Salters and White (1998). Mixtures of asthenosphere (OIB-like components) with continental crust or continentally derived sediments could produce sources that would fall in the low end OIB field with low ^{176}Hf/^{177}Hf and low ^{143}Nd/^{144}Nd for the Tarim basalts.

Li et al. (2008, 2011), Zhang et al. (2008), Zhou et al. (2009) and Tian et al. (2010) suggested that the trace element ratios and Sr–Nd–Pb isotopes and the wide distribution of the basalts of the TLIP support a mantle plume origin. The continuously evolved trend for the $^{87}Sr/^{86}Sr$ and $^{143}Nd/^{144}Nd$ values may imply a continuous magma evolution process for the formation of the Groups 1a, Group 1b and Group 2 basalts during the peak time of a flood-basalt episode, and even extend to those of olivine pyroxenite and diabase in the subsequent late stage of magma evolution.

8. Conclusion

Hf isotopes can provide a further evidence to limit magmatic origin and evolution combined with major and trace elements and Sr–Nd–Pb isotopes generally, but it may not be a good indicator to use for the evaluation of magmatic origin by itself. Based on a detailed study on Hf isotopes, combined with the trace and rare earth elements and Sr–Nd–Pb isotopic compositions of the basalts from the Tarim Basin, the following conclusions can be made.

(1) The $^{176}Hf/^{177}Hf$ isotopic components of the three groups of basalts and intrusive suites range from 0.282584 to 0.282837 and 0.282621–0.282789, respectively. The $\varepsilon Hf(t)$ in the Group 1a, Group 1b and Group 2 basalts, olivine pyroxenite, diabase and syenitic porphyry obtained are -0.4–4.4, 0.5–2.1, 1.9–3.1, 6.0–6.5, 4.5–5.7 and 6.5–8.3, respectively. The low $^{176}Hf/^{177}Hf$, $^{143}Nd/^{144}Nd$ and $^{206}Pb/^{204}Pb$ in Tarim basalts in inferred to reflect the incorporation of partial melts of the lithosphere mantle and melts from the asthenosphere mantle with OIB-like in the early stages of the plume activity in the Early Permian. The Group 1a and Group 1b basalts fall in the same Hf–Nd array, and the Group 2 basalts fall in a separate Hf–Nd array with much higher $\varepsilon Nd(t)$. Olivine pyroxenite, diabase and syenitic porphyry fall in the higher $\varepsilon Nd(t)$ and $\varepsilon Hf(t)$ field, and olivine pyroxenite and diabase are close to OIB-like source with much higher $\varepsilon Nd(t)$ and $\varepsilon Hf(t)$ values than the TLIP basalts. The marked changes of Hf isotopes from the bottom of Kai1 unit to the top of the Kai6 unit basalts further support the operation of the evolved mantle source with the relatively primary magma during the formation of the Yingan section basalts. The Taxinan basalts in the southwestern Tarim Basin have the same Hf isotope comparable to those from Keping area in the northwestern Tarim Basin.

(2) New Hf isotopes together with previous Nd and Pb isotope data support the model that the Tarim basalts were derived from a magma source similar to OIB-like plume source. The evolved magmatic process for the basalts and olivine pyroxenite and diabase occurred in different time under almost the same within-plate setting was suggested. The basalts probably were derived from two end-member sources of lithospheric mantle and asthenosphere (OIB-components), and even plume mantle. The distinction between the basalts and mafic intrusive rocks could reflect the presence of a larger percentage of the pyroxene-rich component in the Bachu mafic–ultramafic source. The new Hf isotopic results provide robust evidence for different sources between the Tarim basalts (285–290 Ma) and the intrusive rocks (274–284 Ma). Furthermore, the $\varepsilon Hf(t)/\varepsilon Nd(t)$ ratios show that the en-echelon arrays for the Tarim basalts and intrusive rocks might correspond to two different periods of magmatic activities in the Tarim Basin during the Early Permian.

(3) The TLIP basalts have comparable $^{176}Hf/^{177}Hf$ and $^{143}Nd/^{144}Nd$ ratios with the basaltic lava of the Pitcairn hotspot. The TLIP basalts have low $\varepsilon Nd(t)$ and moderate $\varepsilon Hf(t)$ ratios, indicating a low $\varepsilon Nd(t)$ and moderate $\varepsilon Hf(t)$ OIB-like source. The $^{176}Hf/^{177}Hf$ and $^{143}Nd/^{144}Nd$ values of the Group 1a and Group 1b basalts of the TLIP basalts are comparable to those from the Karoo high-Ti basalts, and the Group 2 basalts are comparable to those from the Karoo low-Ti basalts and diabase. The slope of the $\varepsilon Hf(t)$-$\varepsilon Nd(t)$ isotopic array and source components from the TLIP Group 1a and Group 1b basalts can be compared to the Karoo CFB basalt (HT), with the former having much higher $\varepsilon Hf(t)$. The TLIP intrusive rocks can be compared to the Siberian LIP meimechite and kimberlite, and Kerguelen Archipelago volcanic rocks. The Tarim Group 1a basalts have similar $\varepsilon Hf(t)$ and $^{206}Pb/^{204}Pb$ components with the high-Ti basalts from the Karoo CFB, particularly Karoo CFB picritic basalts.

In general, the basalts and intrusive rocks from the TLIP might be derived from different componental proportion of magma sources and/or underwent evolved magmatic processes.

Acknowledgements

The authors express sincere thanks to X.-R. Liang, Y. Liu, G.-Q. Hu, and J.-L. Ma of GIGCAS for assistance in Hf isotope analyses, and to the Petroleum Exploration and Development of Tarim Oil Field of China for field work and providing valuable drill hole samples. S.-C. Lai (Northwest University, PR China) and an anonymous reviewer and A.J. Crawford (University of Tasmania, Australia) are appreciated for their constructive comments. This study was financially supported by the National Basic Research Program of China (973 Programs: 2007CB411303 and 2011CB808902) and the National Natural Science Foundation of China (Nos. 40972045, 40930315 and 41072048) and Research Fund for the Doctoral Program of Higher Education of China (20110101110001) and Qianjiang Talents Project of Zhejiang Province of China (2010R10031).

References

Ao, S.J., Xiao, W.J., Han, C.M., Mao, Q.G., Zhang, J.E., 2010. Geochronology and geochemistry of Early Permian mafic-ultramafic complexes in the Beishan area, Xinjiang, NW China: implications for late Paleozoic tectonic evolution of the southern Altaids. Gondwana Research 18, 466–478.

Arndt, N.T., Christensen, U., 1992. The role of lithospheric mantle in continental flood volcanism: thermal and geochemical constraints. Journal of Geophysical Research 97, 10967–10981.

Blichert-Toft, J., Albarède, F., 1997. The Lu–Hf isotope geochemistry of chondrites and the evolution of the mantle-crust system. Earth and Planetary Science Letters 148, 243–258.

Blichert-Toft, J., Albarède, F., 1999. Hf isotopic compositions of the Hawaii Scientific Drilling Project core and the source mineralogy of Hawaiian basalts. Geophysical Research Letters 26, 935–938.

Blichert-Toft, J., White, W.M., 2001. Hf isotope geochemistry of the Galapagos Islands. Geochemistry Geophysics Geosystems 2, 1043. doi:10.1029/2000GC000138.

Blichert-Toft, J., Frey, F.A., Albarède, F., 1999. Hf isotope evidence for pelagic sediments in the source of Hawaiian. Science 285, 879–882.

Campbell, I.H., Griffiths, R.W., 1990. Implications of mantle plume structure for the evolution of flood basalts. Earth and Planetary Science Letters 99, 79–93.

Campbell, I.H., Czamanske, G.K., Fedorenko, V.A., Hill, R.I., Stepanov, V., 1992. Synchronism of the Siberian Traps and the Permian–Triassic boundary. Science 258, 1760–1763.

Carlson, R.W., Hart, W.K., 1987. Crustal genesis on the Oregon Plateau. Journal of Geophysical Research 92, 6191–6206.

Carlson, R.W., Czamanske, G., Fedorenko, V., Ilupin, I., 2006. A comparison of Siberian meimechites and kimberlites: implications for the source of high-Mg alkalic magmas and flood basalts. Geochemistry Geophysics Geosystems 7, Q11014. doi:10.1029/2006GC001342.

Chauvel, C., Blichert-Toft, J., 2001. A hafnium isotope and trace element perspective on melting of the depleted mantle. Earth and Planetary Science Letters 190, 137–151.

Chen, C.Y., Frey, F.A., 1985. Trace element and isotopic geochemistry of lavas from Haleakala volcano, East Maui, Hawaii: Implications for the origin of Hawaiian basalts. Journal of Geophysical Research 90, 8743–8768.

Chen, H.L., Yang, S.F., Dong, C.W., Jia, C.Z., Wei, G.Q., Wang, Z.G., 1997. Confirmation of Permian basite zone in the Tarim basin and its tectonic significance. Geochemica 26, 77–87 (in Chinese with English abstract).

Chen, H.L., Yang, S.F., Wang, Q.H., Luo, J.C., Jia, C.Z., Wei, G.Q., Li, Z.L., He, G.Y., Hu, A.P., 2006. Sedimentary response to the Early–Mid Permian basaltic magmatism in the Tarim plate. Geology in China 33, 545–552 (in Chinese with English abstract).

Chung, S.L., Jahn, B.M., 1995. Plume-lithosphere interaction in generation of the Emeishan flood basalts at the Permian–Triassic boundary. Geology 23, 889–892.

Condie, K.C., 2001. Mantle Plumes and Their Record in Earth History. Cambridge University Press.

Eisele, J., Sharma, M., Galer, S.J.G., Blichert-Toft, J., Devey, C.W., Hofmann, A.W., 2002. The role of sediment recycling in EM-1 inferred from Os, Pb, Hf, Nd, Sr isotope and trace element systematics of the Pitcairn hotspot. Earth and Planetary Science Letters 196, 197–212.

Elkins-Tanton, L.T., Hager, B.H., 2000. Melt intrusion as a trigger for lithospheric foundering and the eruption of the Siberian flood basalts. Geophysical Research Letters 27, 3937–3940.

Ellam, R.M., 2006. New constraints on the petrogenesis of the Nuanetsi picrite basalts from Pb and Hf isotope data. Earth and Planetary Science Letters 245, 153–161.

Ellis, B.S., Barry, T., Branney, M.J., Wolff, J.A., Bindeman, I., Wilson, R., Bonnichsen, B., 2010. Petrologic constraints on the development of a large-volume, high temperature, silicic magma system: the Twin Falls eruptive centre, central Snake River Plain. Lithos 120, 475–489.

Ernst, R.E., Buchan, K.L., 2003. Recognizing mantle plumes in the geological record. Annual Review of Earth and Planetary Sciences 31, 469–523.

Hales, T.C., Abt, D.L., Humphreys, E.D., Roering, J.J., 2005. A lithospheric instability origin for Columbia River flood basalts and Wallowa Mountains uplift in northeast Oregon. Nature 438, 842–845.

Harry, D.L., Leeman, W.P., 1995. Partial melting of melt metasomatized subcontinental mantle and the magma source potential of the lower lithosphere. Journal of Geophysical Research 100, 10255–10269.

Ivanov, A.V., 2007. Evaluation of different models for the origin of the Siberian Traps. Geological Society of America Special Paper 430, 669–691.

Jia, C.Z., 1997. Tectonic Characteristics and Oil-gas, Tarim Basin, China, Beijing. Petroleum Industry Press (in Chinese).

Jiang, C.Y., Zhang, P.B., Lu, D.R., Bai, K.Y., 2004a. Petrogenesis and magma source of the ultramafic rocks at Wajilitag region, western Tarim Plate in Xinjiang. Acta Petrologica Sinica 20, 1433–1444 (in Chinese with English abstract).

Jiang, C.Y., Zhang, P.B., Lu, D.R., Bai, K.Y., Wang, Y.P., Tang, S.H., Wang, J.H., Yang, C., 2004b. Petrology, geochemistry and petrogenesis of the Kalpin basalts and their Nd, Sr and Pb isotopic compositions. Geological Review 50, 492–500 (in Chinese with English abstract).

Jiang, C.Y., Li, Y.Z., Zhang, P.B., Ye, S.F., 2006. Petrogenesis of Permian basalts on the western margin of the Tarim basin, China. Russian Geology and Geophysics 47, 237–248.

Jourdan, F., Bertrand, H., Schärer, U., Blichert-Toft, J., Féraud, G., Kampunzu, A.B., 2007. Major and trace element and Sr, Nd, Hf, and Pb isotope compositions of the Karoo large igneous province, Botswana–Zimbabwe: lithosphere vs mantle plume contribution. Journal of Petrology 48, 1043–1077.

Kempton, P.D., Fitton, J.G., Saunders, A.D., Norwell, G.M., Taylor, R.N., Hardarson, B.S., Pearson, G., 2000. The Iceland plume in space and time: a Sr–Nd–Pb–Hf study of the North Atlantic rifted margin. Earth and Planetary Science Letters 177, 255–271.

King, S.D., Anderson, D.L., 1998. Edge-driven convection. Earth and Planetary Science Letters 160, 289–296.

Li, X.H., Qi, C.S., Liu, Y., Liang, X.L., Tu, X.L., Xie, L.W., Yang, Y.H., 2005. Rapid separation of Hf from rock samples for isotope analysis by MC-ICPMS: a modified single-column extraction chromatography method. Geochemica 34 (2), 109–114 (in Chinese with English abstract).

Li, X.H., Liu, Y., Yang, Y.H., Chen, F.K., Tu, X.L., Qi, C.S., 2007. Rapid separation of Lu–Hf and Sm–Nd from a single rock dissolution and precise measurement of Hf–Nd isotopic ratios for national rock standards. Acta Petrologica Sinica 23, 221–226 (in Chinese with English abstract).

Li, Z.L., Yang, S.F., Chen, H.L., Langmiur, C.H., Yu, X., Lin, X.B., Li, Y.Q., 2008. Chronology and geochemistry of Taxinan basalts from the Tarim Basin: evidence for Permian plume magmatism. Acta Petrologica Sinica 24 (5), 959–970 (in Chinese with English abstract).

Li, Z.L., Chen, H.L., Song, B., Li, Y.Q., Yang, S.F., Yu, X., 2011. Temporal evolution of the Permian large igneous province in Tarim Basin, Northwest China. Journal of Asian Earth Sciences 42, 917–927.

Li, Y.Q., Li, Z.L., Sun, Y.L., Chen, H.L., Yang, S.F., Yu, X., 2010. PGE and geochemistry of Wajilitag ultramafic cryptoexplosive brecciated rocks from Tarim Basin: Implications for petrogenesis. Acta Petrologica Sinica 26, 3307–3318 (in Chinese with English abstract).

Li, Y.Q., Li, Z.L., Sun, Y.L., Santosh, M., Langmuir, C.H., Chen, H.L., Yang, S.F., Yu, X., 2012. Platinum-group elements and geochemical characteristics of the Permian continental flood basalts in the Tarim Basin, Northwest China: implications for the magmatic evolution of the Tarim large igneous province. Chemical Geology (Reviewed).

Li, Z.L., Li, Y.Q., Yang, S.F., Chen, H.L., Langmiur, C.H., Chen, Z.X., Yu, X., 2012. Spatial-geochemical characteristics of the Tarim large igneous province: evidence for mantle plume and lithospheric mantle interaction. Journal of Petrology.

Lightfoot, P.C., Naldrett, A.J., Gorbachev, N.S., Doherty, W., Fedorenko, V.A., 1990. Geochemistry of the Siberian Trap of the Noril'sk area, USSR, with implications for the relative contributions of crust and mantle to flood basalt magmatism. Contributions to Mineralogy and Petrology 104, 631–644.

Lightfoot, P.C., Hawkesworth, C.J., Hergt, J., Naldrett, A.J., Gorbachev, N.S., Fedorenko, V.A., Doherty, W., 1993. Remobilisation of the continental lithosphere by a mantle plume: major-, trace-element, and Sr-, Nd-, and Pb-isotope evidence from picritic and tholeiitic lavas of the Noril'sk District, Siberian Trap, Russia. Contributions to Mineralogy and Petrology 114, 171–188.

Mahéo, G., Blichert-Toft, J., PIN, C., Guillot, S., Pêcher, A., 2009. Partial melting of mantle and crustal sources beneath South Karakorum, Pakistan: implications for the Miocene geodynamic evolution of the India–Asia Convergence Zone. Journal of Petrology 50, 427–449.

Mattielli, N., Weis, D., Blichert-Toft, J., Albarede, F., 2002. Hf isotope evidence for a Miocene change in the Kerguelen mantle plume composition. Journal of Petrology 43, 1327–1339.

Nash, B.P., Perkins, M.E., Christensen, J.N., Lee, D.-C., Halliday, A.N., 2006. The Yellowstone hotspot in space and time: Nd and Hf isotopes in silicic magmas. Earth and Planetary Science Letters 247, 143–156.

Nowell, G.M., Kempton, P.D., Noble, S.R., Fitton, J.G., Saunders, A.D., Mahoney, J.J., Taylor, R.N., 1998. High precision Hf isotope measurements of MORB and OIB by thermal ionisation mass spectrometry: insights into the depleted mantle. Chemical Geology 149, 211–233.

Patchett, P.J., 1983a. Hafnium isotope results from mid-ocean ridges and Kerguelen. Lithos 16, 47–51.

Patchett, P.J., 1983b. Importance of the Lu–Hf isotopic system in studies of planetary chronology and chemical evolution. Geochimica et Cosmochimica Acta 47, 81–91.

Patchett, P.J., Tatsumoto, M., 1980. Hafnium isotope variations in oceanic basalts. Geophysical Research Letters 7, 1077–1080.

Patchett, P.J., Tatsumoto, M., 1981a. The hafnium isotopic evolution of lunar basalts. Lunar and Planetary Science 12, 819–821.

Patchett, P.J., Tatsumoto, M., 1981b. Lu–Hf in chondrites and definition of a chondritic hafnium growth curve. Lunar and Planetary Science 12, 822–824.

Patchett, P.J., Kouvo, O., Hedge, C.E., Tatsumoto, M., 1981. Evolution of continental crust and mantle heterogeneity: evidence from Hf isotopes. Contributions to Mineralogy and Petrology 78, 279–297.

Pirajno, F., Ernst, R.E., Borisenko, A.S., Fedoseev, G., Naumov, E.A., 2009. Intraplate magmatism in Central Asia and China and associated metallogeny. Ore Geology Reviews 35, 114–136.

Rhodes, J.M., 1996. Geochemical stratigraphy of lava flows sampled by the Hawaii Scientific Drilling Project. Journal of Geophysical Research 101, 11,729–11,746.

Richards, M.A., Duncan, R.A., Courtillot, V.E., 1989. Flood basalts and hot-spot tracks: plume heads and tails. Science 246, 103–107.

Salters, V.J.M., 1996. The generation of mid-ocean ridge basalts from the Hf and Nd isotope perspective. Earth and Planetary Science Letters 141, 109–123.

Salters, V.J.M., Hart, S.R., 1991. The mantle sources of ocean islands and arc basalts: the Hf isotope connection. Earth and Planetary Science Letters 104, 364–380.

Salters, V.J.M., White, W.M., 1998. Hf isotope constraints on mantle evolution. Chemical Geology 145, 447–460.

Sharma, M., Basu, A.R., Nesternko, G.V., 1991. Nd–Sr isotopes, petrochemistry, and origin of the Siberian flood basalts, USSR. Geochimica et Cosmochimica Acta 55, 1183–1192.

Tian, W., Campbell, I.H., Allen, C.M., Guan, P., Pan, W.Q., Chen, M.M., Yu, H.J., Zhu, W.P., 2010. The Tarim picrite-basalt-rhyolite suite, a Permian flood basalt from northwest China with contrasting rhyolites produced by fractional crystallization and anatexis. Contributions to Mineralogy and Petrology 160, 407–425.

Turner, S., Hawkesworth, C., 1995. The nature of the sub-continental mantle: constraints from the major-element composition of continental flood basalts. Chemical Geology 120, 295–314.

Turner, S., Arnaud, N., Liu, J., Rogers, N., Hawkesworth, C., Harris, N., Kelley, S., van Calsteren, P., Deng, W., 1996. Post-collision, shoshonitic volcanism on the Tibetan Plateau: implications for convective thinning of the lithosphere and the source of ocean island basalts. Journal of Petrology 37, 45–71.

Vervoort, J.D., Blichert-Toft, J., 1999. Evolution of the depleted mantle: Hf isotope evidence from juvenile rocks through time. Geochimica et Cosmochimica Acta 63, 533–556.

Vervoort, J.D., Patchett, P.J., Blichert-Toft, J., Albarede, F., 1999. Relationships between Lu–Hf and Sm–Nd isotopic systems in the global sedimentary system. Earth and Planetary Science Letters 168, 79–99.

Wang, X.C., Li, X.H., Li, W.X., Li, Z.X., Liu, Y., Yang, Y.H., Liang, X.R., Tu, X.L., 2008. The Bikou basalts in the northwestern Yangtze block, South China: Remnants of 820–810 Ma continental flood basalts? Geological Society of America Bulletin 120, 1478–1492.

Wedepohl, K.H., Baumann, A., 1999. Central European Cenozoic plume volcanism with OIB characteristics and indications of a lower mantle source. Contributions to Mineralogy and Petrology 136, 225–239.

White, R.S., McKenzie, D.P., 1989. Volcanism at rifts. Scientific American 261, 62–71.

Wooden, J.L., Czamanske, G.K., Fedorenko, V.A., Arndt, N.T., Chauvel, C., Bouse, R.M., King, B.-S.W., Knight, R.J., Siems, D.F., 1993. Isotopic and trace-element constraints on mantle and crustal contributions to Siberian continental flood basalts, Noril'sk area, Siberia. Geochimica et Cosmochimica Acta 57, 3677–3704.

Woodhead, J.D., McCulloch, M.T., 1989. Ancient seafloor signals in Pitcairn Island lavas and evidence for large amplitude, small length-scale mantle heterogeneities. Earth and Planetary Science Letters 94, 257–273.

Xiao, L., Xu, Y.G., Chung, S.L., He, B., Mei, H.J., 2003. Chemostratigraphic correlation of upper Permian lavas from Yunnan Province, China: extent of the Emeishan Large Igneous Province. International Geology Review 45, 754–766.

Xiao, W.J., Huang, B., Han, C., Sun, S., Li, J., 2010. A review of the western part of the Altaids: a key to understanding the architecture of accretionary orogens. Gondwana Research 18, 253–273.

Xu, Y.G., Chung, S.L., Jahn, B.M., Wu, G.Y., 2001. Petrologic and geochemical constraints on the petrogenesis of Permian–Triassic Emeishan flood basalts in southwestern China. Lithos 58, 145–168.

Yang, S.F., Chen, H.L., Dong, C.W., Jia, C.Z., Wang, Z.G., 1996. The discovery of Permian syenite inside Tarim basin and its geodynamic significance. Geochemica 25, 121–128 (in Chinese with English abstract).

Yang, S.F., Chen, H.L., Ji, D.W., Li, Z.L., Dong, C.W., Jia, C.Z., Wei, G.Q., 2005. Geological process of early to middle Permian magmatism in Tarim basin and its geodynamic significance. Geological Journal of China Universities 11, 504–511 (in Chinese with English abstract).

Yang, S.F., Li, Z.L., Chen, H.L., Chen, W., Yu, X., 2006a. $^{40}Ar/^{39}Ar$ dating of basalts from Tarim Basin, NW China and its implication to a Permian thermal tectonic event. Journal of Zhejiang University-Science A 7 (Supp. II), 170–174.

Yang, S.F., Li, Z.L., Chen, H.L., Xiao, W.J., Yu, X., Lin, X.B., Shi, X.G., 2006b. Discovery of a Permian quartz syenitic porphyritic dyke from the Tarim Basin and its tectonic implications. Acta Petrologica Sinica 22, 1405–1412 (in Chinese with English abstract).

Yang, S.F., Li, Z.L., Chen, H.L., Santosh, M., Dong, C.W., Yu, X., 2007a. Permian bimodal dyke of Tarim Basin, NW China: geochemical characteristics and tectonic implications. Gondwana Research 12, 113–120.

Yang, S.F., Yu, X., Chen, H.L., Li, Z.L., Wang, Q.H., Luo, J.C., 2007b. Geochemical characteristics and petrogenesis of Permian Xiaohaizi ultrabasic dyke in Bachu area, Tarim basin. Acta Petrologica Sinica 23, 1087–1096 (in Chinese with English abstract).

Yu, X., Chen, H.L., Yang, S.F., Li, Z.L., Wang, Q.H., Lin, X.B., Xu, Y., Luo, J.C., 2009. Geochemical features of Permian basalts in Tarim Basin and compared with Emeishan LIP. Acta Petrologica Sinica 25 (6), 1492–1498 (in Chinese with English abstract).

Yu, X., Yang, S.F., Chen, H.L., Chen, Z.Q., Li, Z.L., Li, Y.Q., 2011. Permian flood basalts from Tarim Basin, Northwest China: SHRIMP zircon U–Pb dating and geochemical characterizations. Gondwana Research 20, 485–497.

Zhang, S.B., Ni, Y.N., Gong, F.H., Lu, H.N., Huang, Z.B., Lin, H.L., 2003. A Guide to the Stratigraphic Investigation on the Periphery of the Tarim Basin. Petroleum Industry Press, p. 280.

Zhang, C.L., Li, X.H., Li, Z.X., Ye, H.M., Li, C.N., 2008. A Permian layered intrusive complex in the Western Tarim Block, Northwestern China: product of a ca. 275-Ma mantle plume. Journal of Geology 116, 269–287.

Zhang, Y.T., Liu, J.Q., Guo, Z.F., 2010. Permian basaltic rocks in the Tarim basin, NW China: implications for plume-lithosphere interaction. Gondwana Research 18, 596–610.

Zhang, C.L., Yang, D.S., Wang, H.Y., Takahashi, Y., Ye, H.M., 2011. Neoproterozoic mafic-ultramafic layered intrusion in Quruqtagh of northeastern Tarim Block, NW China: two phase of mafic igneous activity with different mantle sources. Gondwana Research 19, 177–190.

Zhou, M.F., Zhao, J.H., Jiang, C.Y., Gao, J.F., Wang, W., Yang, S.H., 2009. OIB-like, heterogeneous mantle sources of Permian basaltic magmatism in the western Tarim Basin, NW China: implications for a possible Permian large igneous province. Lithos 113, 583–594.